Highly Redshifted Radio Lines
ASP Conference Series, Vol. 156, 1999
C.L. Carilli, S.J.E. Radford, K.M. Menten, and G.I. Langston (eds)

BIMA and Keck Imaging of the Radio Ring PKS 1830–211[1].

B. L. Frye
Astronomy Department, University of California, Berkeley, CA 94720

F. Courbin
Institut d'Astrophysique et de Géophysique, Université de Liège, Avenue de Cointe 5, B-4000 Liège, Belgium.
URA 173 CNRS-DAEC, Observatoire de Paris, F-92195 Meudon Principal Cédex, France.

T. J. Broadhurst and W. J. W. Welch
Astronomy Department, University of California, Berkeley, CA 94720

C. Lidman
European Southern Observatory, Casilla 19001, Santiago 19, Chile.

P. Magain[2]
Institut d'Astrophysique et de Géophysique, Université de Liège, Avenue de Cointe 5, B-4000 Liège, Belgium.

M. Pahre and S.G. Djorgovski
Palomar Observatory, California Institute of Technology, Pasadena, CA 91125, USA

Abstract. We discuss BIMA (Berkeley Illinois Maryland Association) data and present new high quality optical and near-IR Keck images of the bright radio ring PKS 1830–211. Applying a powerful new deconvolution algorithm we have been able to identify both images of the radio source. In addition we recover an extended source in the optical, consistent with the expected location of the lensing galaxy. The source counterparts are very red, $I - K \sim 7$ suggesting strong Galactic absorption with additional absorption by the lensing galaxy at $z = 0.885$, and consistent with the detection of high redshift molecules in the lens.

1. Introduction

The bright radio source PKS 1830–211 (Jauncey et al. 1991) has attracted much attention as the most detailed example of a lensed radio ring. Of the classically-lensed QSOs, its short time delay of 44 days (van Ommen et al. 1995) and clean lens geometry (e.g. Subrahmanyan et al, 1990; hereafter S90), make it a good candidate for measuring H_0. The lens, a gas rich galaxy at z=0.89, was discovered in the millimeter via molecular absorption (Wiklind & Combes 1996), which is seen towards only one of the two flat spectrum hot spots (Wiklind & Combes 1996, Frye et al. 1997). A nearby saturated M-star and heavy extinction along the line of sight (b = –5.7 degrees, Djorgovski, et al. 1992; hereafter D92) has obscured the lens and the source from identification. In this paper we describe how the MCS deconvolution algorithm (Magain, Courbin

[1]Based on observations obtained at the W.M. Keck Observatory, Hawaii, which is operated jointly by the California Institute of Technology and the University of California.

[2]Maître de Recherches au FNRS (Belgium)

& Sohy, 1997) was used to detect the counterparts of this bright radio ring lens in deep Keck optical and infrared images.

2. Deconvolution

I and K band Keck data were obtained for this study. The details of the observations and reductions are presented in Courbin, et al. 1998. The MCS deconvolution code (Magain, Courbin & Sohy, 1997) was applied to both the optical and IR images. The limiting magnitudes of the images ($3\sigma_{sky}$ integrated over the whole object) are 24.0 in I and 21.3 in K.

The deconvolution process is described in detail by Courbin, Lidman & Magain (1997) and was applied to the present data in an identical manner. As output from the procedure, one gets a deconvolved image, decomposed into point sources and a diffuse background, which is compatible with all the input images included in the data set. The photometry and the astrometry of the point sources are also obtained as byproducts of the deconvolution (see Table 1). Objects near the frame edges are not well-fitted. (e.g. objects labelled 2,3 and 4 in Figure 1). Note that object 1 is never well-fit by a point source and leaves significant residuals after deconvolution. We therefore conclude that it is extended or that it is a very strong blend of point sources.

3. Results

In Fig. 1 we present both the raw and deconvolved images in I and K. In addition ESO J and K' data were taken and are presented in Courbin, et al. 1998. The deconvolved images clearly show one red point source at the position expected for the NE radio source of PKS 1830–211. Another red object is observed close to the position of the SW radio source of the lensed system, but the extended nature of the source and the poor quality of the PSF do not allow us to sort out its morphology. The photometry and astrometry of the field are presented in Tables 1 and 2 and Fig. 2.

The point source at the position of the NE radio source is likely to be the IR counterpart of the NE radio image of PKS 1830–211. With our high signal-to-noise we can show that its shape is compatible with a point source, and its color, $I - K = 6.9$, is much redder than any "normal" star (e.g. Koornneef, 1983). The I-band position is also within the 1σ radio error bars. In Fig. 2 we align all positions with respect to the M-star so that we can compare the different positions measured for the NE and SW components at optical and IR wavelengths.

We spatially-resolved molecular absorption towards the two lensed images in the mm and measured the lensed source separation to be $0\farcs98$ (see Fig. 3). In our optical and IR images the SW component is $0.61 \pm 0.13''$ and $0.85 \pm 0.09''$ away from the NE component respectively. A plausible explanation for the apparent positional shift between the optical, IR and radio positions is that the SW component is a blend of two objects: the lensing galaxy and the heavily reddened SW component seen in the radio images.

The flux ratio between the two lensed images of the source is 1 in the I band and < 20 in K. The combination of a reddened SW radio source plus

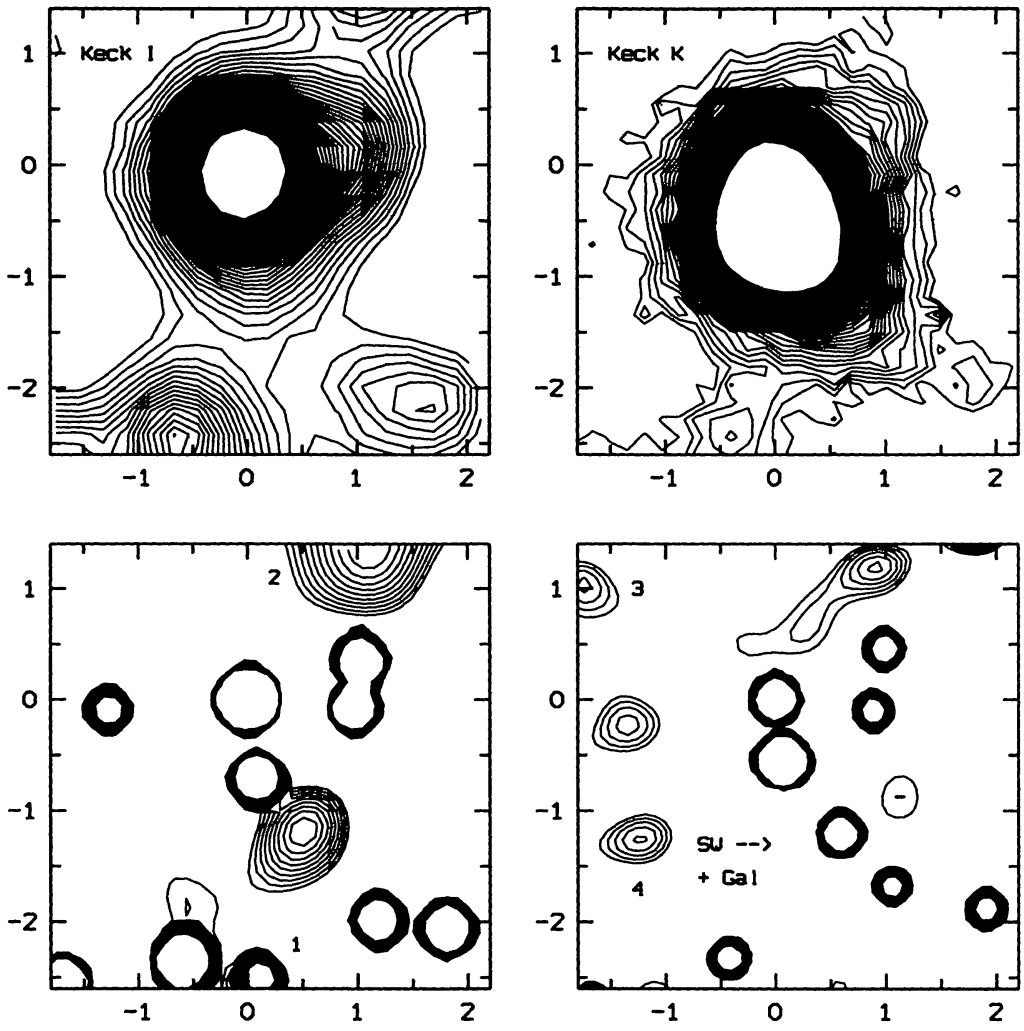

Figure 1. Top row, from left to right: 1. Field of 4.0″ around PKS 1830–211 observed with Keck II in the I-band. This image is a stack of 6 frames with a pixel size of 0.″215 and seeing of 0.″8. 2. Mean of 5 K-band images obtained with Keck I and NIRC. The pixel size is 0.″157 and the seeing is 0.″7. Bottom row, from left to right: 1. Simultaneous deconvolution of the 6 I-band frames: resolution of 0.″215 and pixel size of 0.″1075. 2. Deconvolution of the mean of 5 NIRC images: resolution of 0.″157 and pixel size of 0.″0785. In all the images North is up, East left. The M-star, the NE QSO component candidate and the blended SW component + lensing galaxy candidate are detected. The scale is given in arcseconds relative to the M-star. The NE QSO is directly south of the M-star.

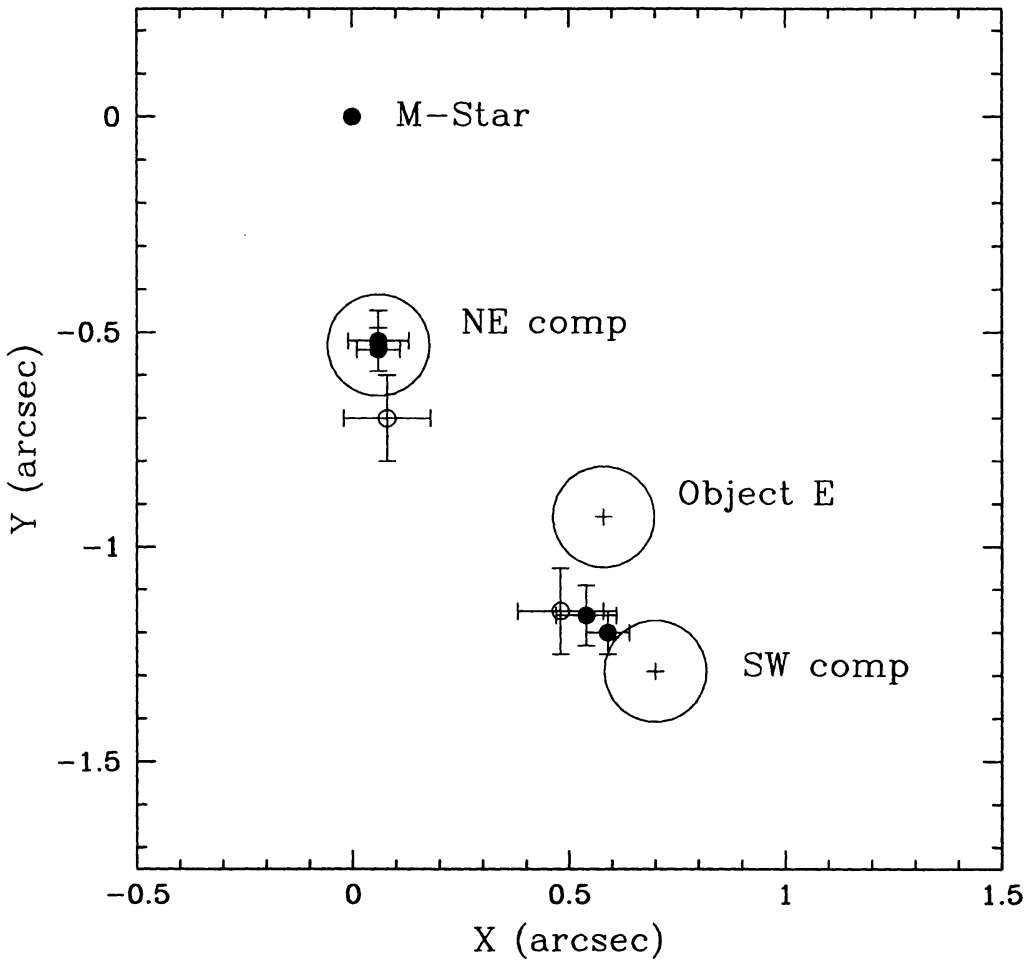

Figure 2. Positions observed for the different objects detected in the optical and near-IR along with their 1σ error bars, relative to the M star. The large open circles show the geometry of the system in the radio. Their radius corresponds to the error bars quoted by S90. The black dots are from the near-IR images while the open circles indicate the result obtained from the I-band data.

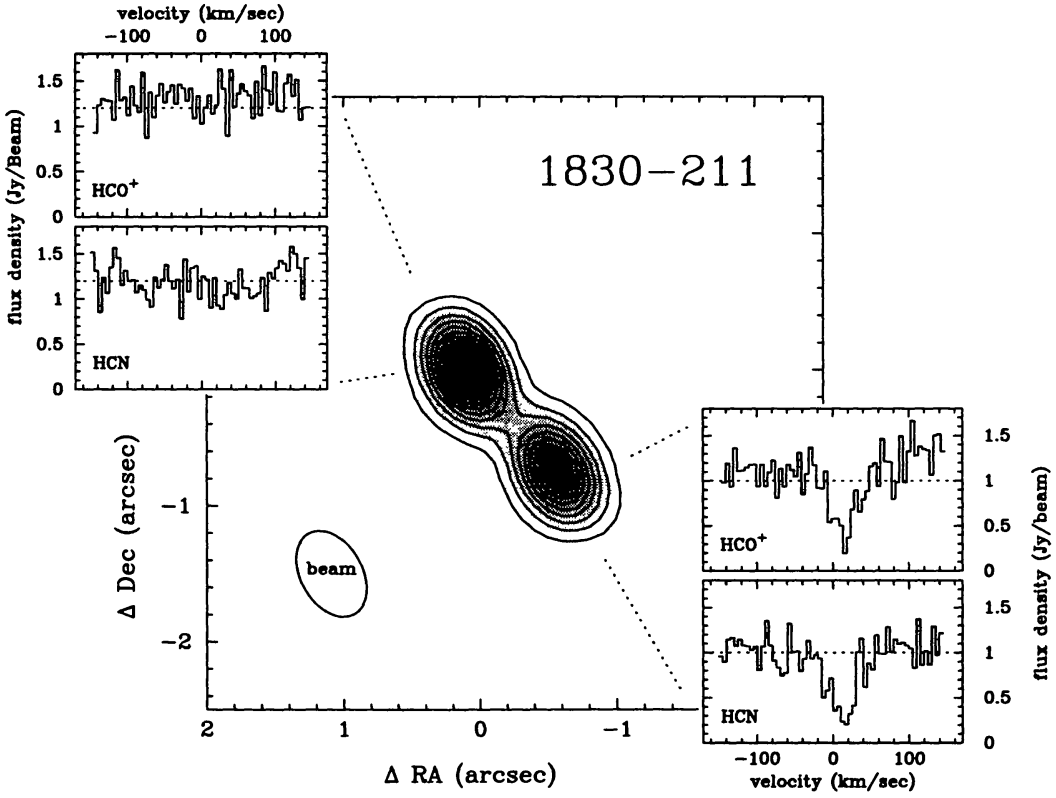

Figure 3. The 3 mm continuum map (center) showing the known double lensed structure is well resolved with a separation of 0.″98 and a flux ratio of 1.14 ± 0.05. Contour levels are spaced by 0.1 Jy/beam with the lowest value at 0.1 Jy/beam. The synthesized beamwidth is 0.″68 × 0.″45 (lower left), where the asymmetry is due to the low elevation of the source as seen from the northern latitude of BIMA. The spectral range covers the redshifted HCN(2-1) and HCO^+(2-1) molecular transitions at 5 km/s resolution, which are shown (inset) for both images. The molecular absorption is detected only in the SW component and does not reach the base of the continuum. Since the two images are similarly bright, the lack of absorption in the NE spectrum confirms that the spill over between the two images is negligible.

Table 1. Summary of the photometry and astrometry for the NE component and the SW component of the lensed source (plus lensing galaxy), and photometry for the M-star.

	M-star	NE Comp.	SW Comp.+Lens
I	19.3 ± 0.1	22.0 ± 0.2	22.3 ± 0.3
K	16.6 ± 0.2	15.1 ± 0.1	18.2 ± 0.2
x(I)		$+0.08 \pm 0.01$	$+0.48 \pm 0.1$
y(I)		-0.70 ± 0.01	-1.15 ± 0.1
x(K)		$+0.06 \pm 0.01$	$+0.59 \pm 0.05$
y(K)		-0.54 ± 0.01	-1.20 ± 0.05

blue lens can explain the large flux ratios. Both NE and SW components are reddened, making PKS 1830–211 another good example of a dusty lens, along with MG 0414+0534 (e.g. Annis & Lupino, 1993) and MG1131+0456 (Larkin et al. 1994), the mean galactic extinction being far below the values considered for PKS 1830–211.

4. Discussion

The main result of our study is the detection of the optical and near-IR counterpart to the NE radio source of PKS 1830-211 and the possible detection of the SW component and lensing galaxy. However, our SW component candidate might be the lensing galaxy alone (its position is also in good agreement with the predictions from the models calculated by S90 and Nair, Narasimha & Rao, 1993) or, given the crowding in the field, a red galactic object almost coincident with the position of the SW radio source. The hypothesis of a demagnified third image of the source (S90) between the 2 main lensed images is unlikely as in such a case extinction of the lens would have made it visible in the IR. Furthermore, the IR centroid of the SW component would have been shifted towards "object E" rather than to the radio position of the SW component.

The higher contrast between the NE component and nearby M-star in the infrared make near-IR spectroscopy necessary for finding the source z. Deep, high resolution near-IR imaging is needed to reveal the exact nature of the faint SW component. However, even at the highest resolution attainable, 0.″2- 0.″3 in the IR with HST (in particular in K where the SW component of PKS1830-211 is best visible), deconvolution will be essential to discriminate between the SW component candidate, the lensing galaxy and additional faint galactic stars.

Acknowledgments. We thank Hy Spinrad for useful discussions and Dick Plambeck for help with reducing the BIMA data. The expert help of the staff at ESO and WMKO during the observing runs was very much appreciated. FC is supported by ARC 94/99-178 "Action de Recherche Concertée de la Communauté Francaise" and Pôle d'Attraction Interuniversitaire P4/05 (SSTC, Belgium). SGD and MAP acknowledge support from the NSF PYI award AST-9157412.

References

Annis J.E., Luppino G., 1993, ApJ 407, L69

Combes F., Wiklind T., 1997, preprint astro-ph/9711184

Courbin F., Lidman, C., Frye, B., Magain, P., Broadhurst, T. J., Pahre, M, and Djorgovski, S. G. 1998, submitted.

Courbin F., Lidman C., Magain P. 1998, A&A,330, 57.

Djorgovski G.S., Meylan G., Klemola A., Thompson D.J., Weir W.N., Swarup G., Rao A.P., Subrahmanyan R., Smette A. 1992 MNRAS 257, 240

Frye B.L., Welch W.J.W., & Broadhurst T.J., 1997, ApJ 478 L25

Jauncey D.L., Reynolds J.E., Tzioumis A.K., et al. 1991, Nature 352, 132

Koornneef J., 1983, A&A 128, 84

Larkin J.E., Matthews K., Lawrence C.R., 1994, ApJ 420, L9

Magain P., Courbin F., Sohy S. 1997 ApJ, in press; also SISSA preprint astro-ph/9704059

Nair S., Narasimha D., Rao A.P. 1993, ApJ 407, 46

Subrahmanyan R., Narasimha D., Rao P., Swarup G. 1990, MNRAS 246, 263

van Ommen T.D., Jones D.L., Preston R.A., Jauncey D. L. 1995, ApJ 444, 561

Wiklind T., & Combes F. 1996, Nature 379, 139